Journal of Engineering and Science Research 1 (2): 101-109, 2017
e-ISSN: 2289-7127

DOI: 10.26666/rmp.jesr.2017.2.17

Modeling and Simulation of a Fiber Optic Dual Mach-Zehnder Interferometric Intrusion Detection System

Tsung-En Wu[1], *Tai-Lang Jong*[1] *and Chi-Wen Hsieh*[2]
[1]Dept. of Electrical Engineering, National Tsing Hua University,
101, Section 2, Kuang-Fu Road, Hsinchu, 30013, Taiwan (R.O.C.)
[2]Dept. of Electrical Engineering, National Chiayi University,
300 Syuefu Rd., Chiayi City 60004, Taiwan (R.O.C.)

Abstract: This paper aims to provide an overview of the dual Mach-Zehnder interferometric perimeter intrusion detection system (DMZIPIDS), propose a simulation model for the system, and give advice on the design of the system in accordance with simulation results. In this paper, the basic optical phase modulation mechanisms in optical fibers are described at first to clearly elaborate how the system works. Then, an introduction to the system, including its system structure, theory of operation, and noise sources as well as polarization-induced effects in the system, is described. A noise-involved and MATLAB-based simulation model of the system is proposed in order to predict the performance and study the characteristics of the system. Simulation results are presented and discussed.

Key words: *fiber optic sensing, perimeter intrusion detection system, Mach-Zehnder interferometric sensor.*

INTRODUCTION

A perimeter intrusion detection system (PIDS) is a device deployed in an outdoor environment at the boundaries or around sensitive areas, such as airport, nuclear power plants, oil refineries, power stations, prisons, and international borders, in order to monitor, detect, and locate intruders in real time for security assessment and reaction. Various techniques such as infrared [1], radar [2], microwave [3], electric fence [4], accelerometer [5], and fiber optic have been adopted to implement the PIDS. Among them, PIDSs using fiber optic interferometric sensors are of interest since they have plenty advantages, such as lightweight, immunity to electromagnetic interference and multiplexing, high-temperature performance, low energy requirement, high corrosion resistance, high environmental resistance, high sensitivity, water proof, and so on.

A number of studies regarding to PIDSs based on fiber optic sensors have been reported in the literature. For instance, phase-sensitive optical time domain reflectometer (□–OTDR) and scattering effects based sensors[6-7] as well as fiber optic interferometric sensors such as merged Sagnac-Michelson interferometric sensors [8], dual Sagnac interferometric sensors [9-10], and Mach-Zehnder interferometric sensors [11-13] are used to detect and even locate intruders by sensing vibration. In general, at least two reverse transmitted fiber optic interferometers are used for locating intruders by using some time delay estimation (TDE) techniques. However, □–OTDR and scattering effects based sensors use some different methods to locate intruders. This paper uses a dual Mach-Zehnder interferometer (DMZI) architecture to construct the PIDS. Firstly, a fiber optic dual Mach-Zehnder interferometric perimeter intrusion detection system (DMZIPIDS) is described and analyzed. Various noise sources in the system are discussed. A noise-involved and MATLAB-based simulation model of the DMZIPIDS is then proposed. Some advices on the design of the system are given in accordance with simulation results.

Corresponding Author: Tai-Lang Jong, Nat'l Tsing Hua Univ., 101, Section 2, Kuang-Fu Road, Hsinchu, 30013, Taiwan (R.O.C.), 011-886-3-5742577

MODELING AND ANALYSIS

The Mach-Zehnder Interferometer

Figure 1 shows an all-fiber Mach-Zender interferometer. Assume that in ideal case there are neither optical loss nor noise of any sort, the optical fields at one output of the Mach-Zehnder interferometer originating from the two arms, named arm 1 and arm 2 are then

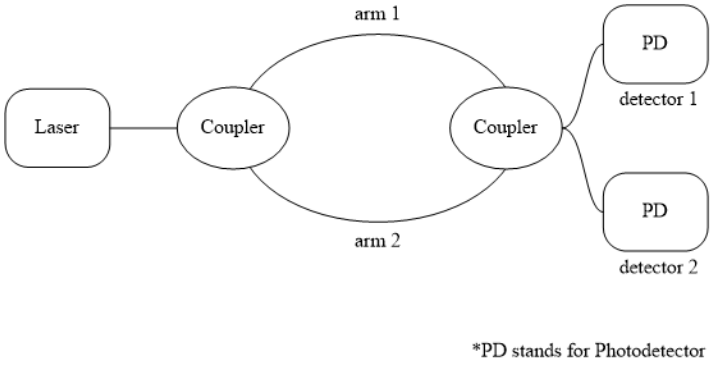

Figure 1 All-fiber Mach-Zehnder interferometer.

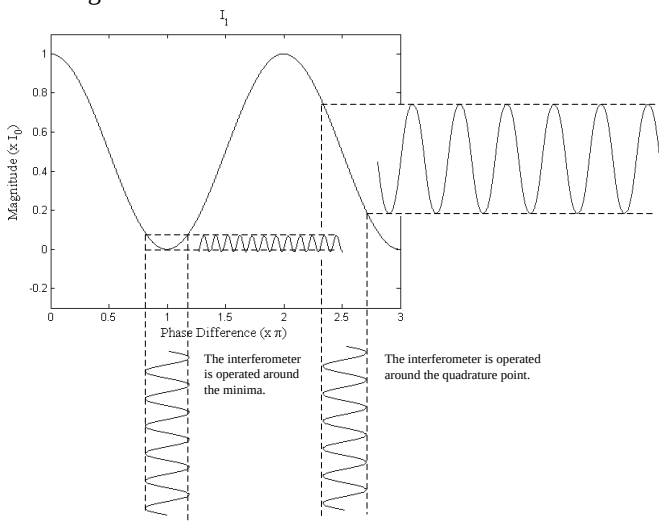

Figure 2 Signal fading problem in the MZI

$$E_1 = \frac{E_0}{2}\cos(\omega \cdot t + \phi_1)$$

and

$$E_2 = \frac{E_0}{2}\cos(\omega \cdot t + \phi_2),$$

where E_0 and ω are optical field and angular frequency of the input light, respectively, $\phi_1$and ϕ_2 are optical phase delay of light traveling through arm 1 and arm 2, respectively. Consequently, the output intensity of the Mach-Zehnder interferometer can be expressed as

$$I = \langle E_1^2 \rangle + \langle E_2^2 \rangle + 2\langle E_1 E_2 \rangle,$$

where $\langle \cdot \rangle$ indicates a time average over a period much greater than $2\pi/\omega$.So the output intensities detected by the two detectors, named detector 1 and detector 2, are given by

$$I_1 = I_0 \cos^2(\frac{\phi_1 - \phi_2}{2}) = \frac{I_0}{2}(1 + \cos\Delta\phi)$$

And

$$I_2 = I_0 \sin^2(\frac{\phi_1 - \phi_2}{2}) = \frac{I_0}{2}(1 - \cos\Delta\phi),$$

where I_0 is the intensity of the input light and $\Delta\phi = \phi_1 - \phi_2$ be the phase difference between the two arms. If one of two arms (or both two arms) is exposed to some external influences, then the optical phase of the light is modulated by the environmental field to be detected. Assume that the phase difference between the two arms are divided into a signal of amplitude ϕ_s and angular frequency ω and a slowly varying phase shift ϕ_d, i.e., $\Delta\phi = \phi_d + \phi_s \sin\omega t$, then

$$I_1 = \frac{I_0}{2}(1+\cos(\phi_d + \phi_s \sin\omega \cdot t))$$

Depending on ϕ_d and ϕ_s, signal fading problem could occur as illustrated in figure 2.

The DMZIPIDS

Figure 3 depicts the schematic diagram of DMZIPIDS. The light from the laser is polarization controlled, split equally by a coupler and input to the dual Mach-Zehnder interferometer (DMZI). Two beams of light then propagate in opposite directions and interference at the end coupler respectively. To be specific, one beam of light travels along the path 1→2→3→4 (CW), which is in clockwise direction. While another beam of light travels along the path a→b→c→d (CCW), which is in counter-clockwise direction. Finally, the interference signals are detected by two photodetectors, sampled and processed by the data acquisition system (DAS). Figure 3(b) shows that an optical fiber cable which contains four optical fibers is used to implement DMZIPIDS. Two of four optical fibers in the cable are selected to be the sensing arms of the MZIs. Depicted in figure 4 shows the optical cable of the interference region of DMZIPIDS mounting on a fence.

Intruders who try to cross over the fence at the event position may cause significant signal at the outputs due to the vibration of fence. This signal is then detected by the system. As can be seen from figure 3(a), assume that the length of the interference region is *L*. The length between the point 3 (or point b, which is the start of the interference region) and the event position is *x*. As a result, the interference signals travel along counterclockwise and clockwise paths to the two photodetectors with the length of *x* and $2L–x$, respectively. The desired time delay *D* between the two interference signals can be expressed as

$$D = \frac{2L - x}{c/n} - \frac{\mathrm{x}}{c/n},$$

where *n* is the refractive index of the optical fiber and *c* is the speed of light in vacuum. The event position *x* can be calculated from the estimated time delay $\hat{D}$ that is close to *D*, thus "locate" the intruders. To locate intruders in the presence of noises and polarization-induced effects in the output signals, accurately is another important challenge of DMZIPIDS. Noises and polarization-induced effects that appear in the output signals may affect the positioning accuracy and positioning error severely thus degrades the performance of DMZIPIDS. They may as well make it hard to discriminate between nuisance events and intrusion events.

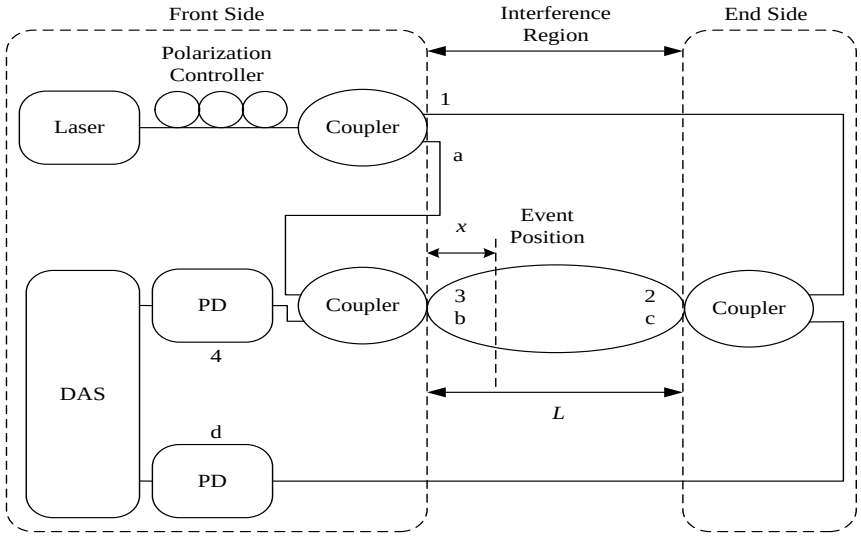

*DAS stands for data acquisition system

*PD stands for Photodetector

(a)

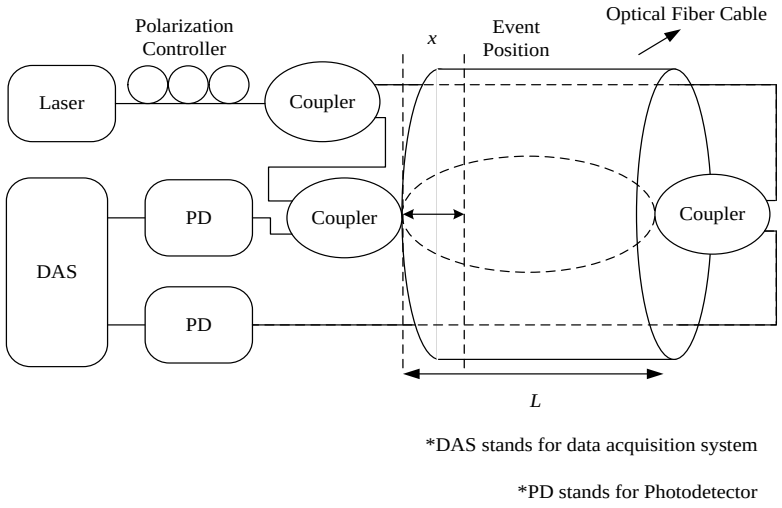

(b)

Figure 3(a) Schematic diagram of DMZIPIDS; (b) Use of a single fiber cable to implement DMZIPIDS. [14]

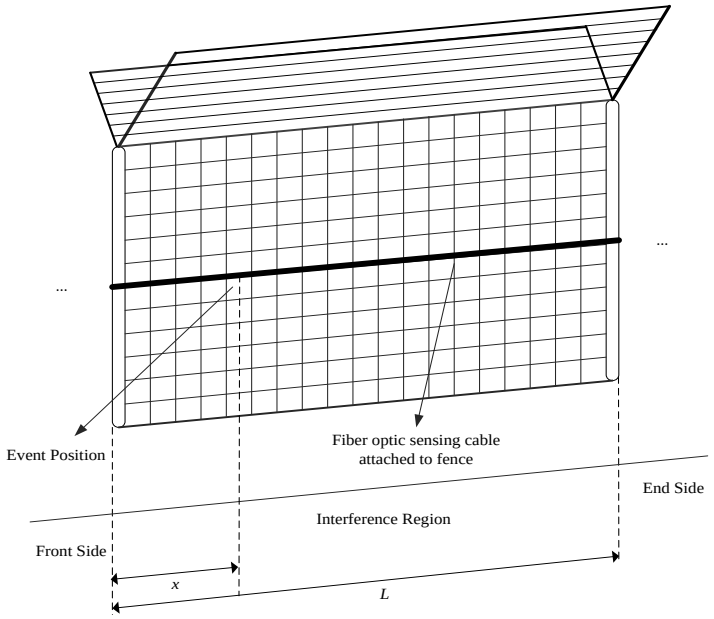

Figure 4 Implementation of DMZIPIDS on a fence.

Noise Model of the DMZIPIDS

The noise sources in the DMZIPIDS may come from electronics thermal noise, electronics shot noise, transimpedance circuit noise, laser's optical intensity noise, optical phase noises due to frequency instability of laser and optical phase noise due to thermal drifts, and environmental perturbations induced phase noise. Polarization-induced effects include polarization-induced phase shift (PIPS) and polarization-induced fading (PIF) [15]. PIPS and PIF in the MZI occurs due to two sources of polarization wandering: that in the two arms of the interferometer itself and that occurring in the input fiber, which changes the input SOP of the light, to the system. It can be shown that

$$\begin{cases} I_{CW} = \frac{I_0}{2}(1+V_{CW}\cos(\Delta\phi_{CW}-\gamma_{CW})) \\ I_{CCW} = \frac{I_0}{2}(1+V_{CCW}\cos(\Delta\phi_{CCW}-\gamma_{CCW})) \end{cases}$$

where γ_{CW}, γ_{CCW} are the PIPS generated, and V_{CW}, V_{CCW} are the polarization-induced visibility change.

For DMZIPIDS with zero retardation, then $\gamma_{CW} = \gamma_{CCW} = 0$ in ideal case. There are no polarization-induced effects present. But in practice, γ_{CW} and γ_{CCW} may not

be equal, which would cause the positioning error of DMZIPIDS.

In summary, the general noise-involved model of interference signal in DMZIPIDS can be expressed as

$$I(t) = I_0\alpha \cdot [1+n_I(t)] \cdot \{1 \pm n_a(t) \cdot \cos[f(t)+n_\varepsilon(t)+n_p(t)+n_e(t)]\}$$

where I_0 is the intensity of the laser, α is the optical loss, $n_I(t)$ is the intensity noise of the laser, $f(t)$ is the phase difference between the two arms of the interferometer caused by intrusion perturbation, $n_a(t)$ and $n_\varepsilon(t)$ are the visibility and phase noise caused by

PIF and PIPS, $n_p(t)$ is the phase noise of the laser, and $n_e(t)$ is the phase noise caused by environment perturbations.

Therefore, the general noise-involved time delay model of interference signals in DMZIPIDS of interest is given by

$$I_1(t) = I_0\alpha_1[1+n_{1I}(t)] \cdot \{1+n_{1a}(t) \cdot \cos[f(t)+n_{1\varepsilon}(t)+n_{1p}(t)+n_{1e}(t)]\}$$

$$I_2(t) = I_0\alpha_2[1+n_{2I}(t)] \{1+n_{2a}(t) \cdot \cos[f(t-D)+n_{2\varepsilon}(t)+n_{2p}(t)+n_{2e}(t)]\}$$

$$D = \frac{2L-x}{c/n} - \frac{x}{c/n},$$

where L is the physical length of the interference region, x is the length between the starting point of the interference region and the event position (from now on, the convention of the number line is followed such that x is defined to be the event position), c is the velocity of light in vacuum, n is the refractive index of the optical fiber, D is the desired time delay between $I_1(t)$ and $I_2(t)$. It should be noted that the phase noises $n_\varepsilon(t)$, $n_p(t)$, and $n_e(t)$ are indistinguishable from $f(t)$ such that in order to obtain an estimated time delay $\hat{D}$ that is close to D, $n_\varepsilon(t)+n_p(t)+n_e(t)$ must be close to 0.

The intensity outputs of DMZIPIDS are to be converted to electrical currents by photodetectors. Thus, the time delay model represented by photocurrents is given by

$$i_1(t) = \kappa I_0\alpha_1[1+n_{1I}(t)]\{1+n_{1a}(t) \cdot \cos[f(t)+n_{1\varepsilon}(t)+n_{1p}(t)+n_{1e}(t)]\}+i_{1c}(t)$$

$$i_2(t) = \kappa I_0\alpha_2[1+n_{2I}(t)]\{1+n_{2a}(t) \cdot \cos[f(t-D)+n_{2\varepsilon}(t)+n_{2p}(t)+n_{2e}(t)]\}+i_{2c}(t)$$

where κ is the responsivity of the photodetectors; $i_c(t)$ is the total electronics current noises that is additive.

By using the transimpedance amplifier to convert the current into voltage, the time delay model represented by voltage is given by

$$V_1(t) = R_f\kappa I_0\alpha_1[1+n_{1I}(t)]\{1+n_{1a}(t) \cdot \cos[f(t)+n_{1\varepsilon}(t)+n_{1p}(t)+n_{1e}(t)]\}+V_{1c}(t)$$

$$V_2(t) = R_f\kappa I_0\alpha_2[1+n_{2I}(t)]\{1+n_{2a}(t) \cdot \cos[f(t-D)+n_{2\varepsilon}(t)+n_{2p}(t)+n_{2e}(t)]\}+V_{2c}(t)$$

where $V_{1c}(t)$ and $V_{2c}(t)$ represent the RMS value of the total electronics voltage noise.

Finally, in order to simulate DMZIPIDS, assume that the model of the phase difference between the two arms of the interferometer caused by the intrusion event is in the form of

$$f(t) = \phi_d(t) + \sum_{i=1}^{N} \phi_{s_i} \cdot \sin(\omega_i \cdot t) \cdot e^{-t/\tau_i}$$

SIMULATION

To estimate the intrusion location in the simulation and experiment of the DMZIPIDS, Four time delay estimation (TDE) techniques are used, namely cross-correlation (CC), phase transform (PHAT), maximum likelihood (ML), and average squared difference function (ASDF).Based on the laser and electronic components used in building the DMZIPIDS, the pertinent noise models for laser intensity noise, electronics thermal, shot noise, and Opamp electronic noise can be found from the datasheets. Table 1 lists the values of the parameters used in the model of DNZIPIDS. Figure 5 shows the simulated relative intensity noise of laser, electronics thermal noise,

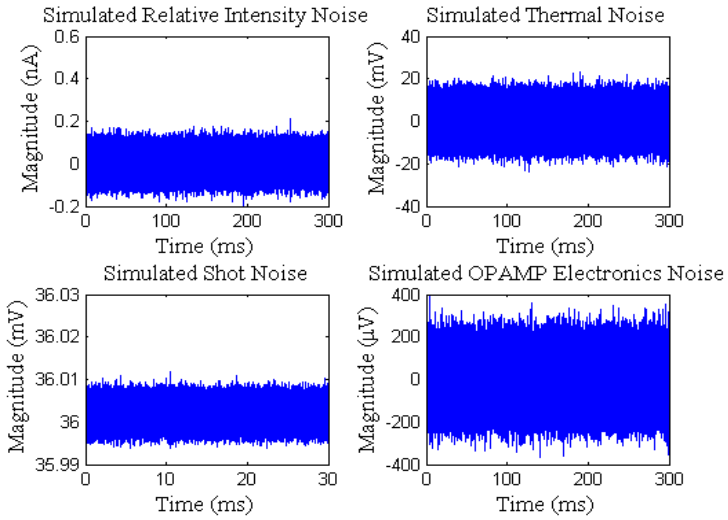

Figure 5 Simulated relative intensity noise of laser, thermal noise, shot noise, and OPAMP electronics noise.

shot noise, and Opamp electronics noise accordingly. It should be noted that the electronics shot noise is simulated using Poisson process, while other noises are simulated as white Gaussian noise.

Various noise corruption scenarios under different phase difference $f(t)$ caused by intrusion are simulated. In each simulation case, due to the randomness, 100 sets of involved noise and intrusion location (or equivalently, the time delay D) are randomly generated and V_1 and V_2 signals are processed accordingly to estimate the time delay. Since the electronics noise is wideband, simulations are also conducted by passing V_1 and V_2 through a predesigned lowpass filter before time delay estimation. Some of the simulation results are illustrated below. Table 2 shows the effect of electronics noise corruption on the mean and standard deviation of time delay estimation error by the four methods (in term of number of samples) under different SNR situations ($I_0\alpha$(μW)/electronic noise power) for $f(t) = 0.5\pi+\sin(2\pi\cdot300\cdot t)\cdot e^{-t/0.05}$.It can be seen that the time-domain TDE methods (CC and ASDF) yield better results than the frequency-domain TDE methods (ML and PHAT) in this situation. If the detector signalsV_1 and V_2 are lowpass filtered before the TDE, then all four methods yield the near perfect time delay estimation results as shown in table 3.

Table 4 lists the effect of environmental induced phase noise (White Gaussian) and electronics noise on the mean and standard deviation of time delay estimation error by the four methods under different RMS value of phase noise for $f(t) = 0.5\pi+\sin(2\pi\cdot300\cdot t)\cdot e^{-t/0.05}$. Again, the time-domain TDE methods (CC and ASDF) yield better results than the frequency-domain TDE methods (ML and PHAT) in this situation. If the detector signals V_1 and V_2 are lowpass filtered before the TDE, then all four methods yield the near perfect time delay estimation results as shown in table 5.

Table 1 The values of the parameters used in the model of DNZIPIDS.

Parameter		Type	Units
Received Light Intensity	$I_0\alpha$	6	□W
Responsivity of Photodetectors	κ	0.9	A/W
Dark Current of Photodetectors	i_{dark}	0.6	nA
Feedback Resistance of TIA	R_f	500	KΩ
Total Feedback Shunt Capacitance of TIA	C_f	5	pF
Total Input Shunt Capacitance. of TIA	C_i	1.4	pF
Input Current Noise Density of Opamp	i_n	10	fA/$\sqrt{\text{Hz}}$
Input Voltage Noise Density of Opamp	e_n	5.8	nV/$\sqrt{\text{Hz}}$

Gain–Bandwidth Product of Opamp	*GBW*	90	MHz
RMS Value of Thermal Voltage Noise	V_{th}	5	mV
RMS Value of Shot Voltage Noise	V_{sn}	36	mV
RMS Value of Input Current Voltage Noise of Opamp	V_{in}	1.58	μV
RMS Value of Input Voltage Voltage Noise of Opamp	V_{en}	78	μV
RMS Value of Total Electronics Voltage Noise	V_c	36.35	mV
Length of Interference Region	L	40	km
Velocity of Light in Vacuum	c	3	10^8 m/s
Refractive Index ofOptical Fiber	n	1.444	
Sampling Rate of DAS	F_s	2	MS/s

Table 2 Mean and std of estimated time delay error vs. $I_0\alpha$. $V_1(t)$ and $V_2(t)$ are corrupted by electronics noises under $f(t) = 0.5\pi + \sin(2\pi \cdot 300 \cdot t) \cdot e^{-t/0.05}$.

$I_0\alpha$(μW) /Mean of SNR	CC		PHAT		ML		ASDF	
	mean	std	mean	std	mean	std	mean	std
6 / 37.45	3.62	3.27	156.96	232.96	156.96	232.96	4.27	3.27
5 / 35.87	4.01	3.69	157.54	232.64	157.54	232.64	4.54	3.43
4 / 33.93	5.01	4.35	180.76	248.8	180.76	248.8	5.26	4.06
3 / 31.43	6.5	5.35	183.17	254.11	183.17	254.11	6.75	5.27
2 / 27.91	9.13	7.62	175.32	257.91	175.32	257.91	9.36	7.35
1 / 21.89	18.29	15.49	131.37	233.35	131.37	233.35	19.86	14.77

Table 3 Mean and std of estimated time delay error vs. $I_0\alpha$. Same condition but with V_1, V_2 lowpass filtered before time delay estimation.

$I_0\alpha$(μW) /Mean of SNR	CC		PHAT		ML		ASDF	
	mean	std	mean	std	mean	std	mean	std
6 / 37.45	0	0	0	0	0	0	0	0
5 / 35.87	0	0	0	0	0	0	0	0
4 / 33.93	0	0	0	0	0	0	0	0
3 / 31.43	0	0	0	0	0	0	0	0
2 / 27.91	0	0	0	0	0	0	0	0
1 / 21.89	0.85	0.94	0	0	0	0	0.85	0.94

Table 4 Mean and std of estimated time delay error vs. RMS values of phase noise. $V_1(t)$ and $V_2(t)$ are also corrupted by electronics noises under $f(t) = 0.5\pi + \sin(2\pi \cdot 300 \cdot t) \cdot e^{-t/0.05}$.

RMS Values of Phase Noise (rad)	CC		PHAT		ML		ASDF	
	mean	std	mean	std	mean	std	mean	std
0	3.9	3.38	195	270.25	195	270.25	4.2	2.96
0.2	13.14	10.37	199.3	267.44	199.3	267.44	14.27	10.75
0.4	19.25	17.62	177.85	250.68	177.85	250.68	20.24	15.56

0.6	28.82	24.58	188.25	232.33	188.25	232.33	30.27	22.86
0.8	26.68	26.07	169.85	210.87	169.85	210.87	32.06	27.69
1	34.46	32.71	183.82	219.39	183.82	219.39	39.57	31.48

Table 5 Mean and std of estimated time delay error vs. RMS values of phase noise. Same condition but with V_1, V_2 lowpass filtered before time delay estimation.

RMS Values of Phase Noise (rad)	CC		PHAT		ML		ASDF	
	mean	std	mean	std	mean	std	mean	std
0	0	0	0	0	0	0	0.01	0.1
0.2	0.01	0.1	0	0	0	0	0.02	0.14
0.4	0.02	0.2	0	0	0	0	0.03	0.22
0.6	0.32	1.7	0	0	0	0	0.33	1.7
0.8	1.15	5.39	0	0	0	0	1.16	5.39
1	0.82	5.19	0	0	0	0	0.83	5.19

CONCLUSION

To conclude, electronics noises and environmental perturbations induced phase noises can typically be modeled as white Gaussian noises. The interference signals of DMZIPIDS that are corrupted by these noises can be reconstructed by using a digital lowpass filter.

The simulation results show that after filtering the positioning errors approach 0 and positioning accuracies approach 100%. However, some other noises such as polarization-induced phase noise and phase noise caused by laser instability cannot be modeled as white Gaussian noise. These phase noises are indistinguishable from $f(t)$ thus lead to positioning errors of DMZIPIDS. To improve the performance of DMZIPIDS, such phase noises must be alleviated or even eliminated.

ACKNOWLEDGMENTS

The authors acknowledge the financial support from Ministry of Science and Technology (MOST), Taiwan (R.O.C.) under project no. 105-2221-E-007-117-.

REFERENCES

[1]H. J. Keller, "Advanced passive infrared presence detectors as key elements in integrated security and building automation systems," in *Security Technology, 1993. Security Technology, Proceedings. Institute of Electrical and Electronics Engineers 1993 International Carnahan Conference on*, 1993, pp. 75-77.

[2]P. Weber, A. Premji, T. J. Nohara, and C. Krasnor, "Low-cost radar surveillance of inland waterways for homeland security applications," in *Radar Conference, 2004. Proceedings of the IEEE*, 2004, pp. 134-139.

[3]M. Peichl, S. Dill, M. Jirousek, and H. Suess, "Passive microwave remote sensing for security applications," in *Radar Conference, 2007. EuRAD 2007. European*, 2007, pp. 32-35.

[4]M. Leblond, C. Dussault, J. P. OUELLET, M. Poulin, R. Courtois, and J. Fortin, "Electric Fencing as a Measure to Reduce Moose-Vehicle Collisions," *The Journal of wildlife management*, vol. 71, pp. 1695-1703, 2007.

[5]A. Yousefi, S. Member, A. Dibazar, and T. Berger, "Intelligent fence intrusion detection system: detection of intentional fence breaching and recognition of fence climbing," in *Technologies for Homeland Security, 2008 IEEE Conference on*, 2008, pp. 620-625.

[6]Y. Lu, T. Zhu, L. Chen, and X. Bao, "Distributed vibration sensor based on coherent detection of phase-OTDR," *Lightwave Technology, Journal of*, vol. 28, pp. 3243-3249, 2010.

[7]J. C. Juarez, E. W. Maier, K. N. Choi, and H. F. Taylor, "Distributed fiber-optic intrusion sensor

system," *Journal of lightwave technology*, vol. 23, p. 2081, 2005.

[8]S. J. Spammer, P. L. Swart, and A. A. Chtcherbakov, "Merged Sagnac-Michelson interferometer for distributed disturbance detection," *Lightwave Technology, Journal of*, vol. 15, pp. 972-976, 1997.

[9]M. Zyczkowski, M. Szustakowski, N. Palka, and M. Kondrat, "Fiber optic perimeter protection sensor with intruder localization," in *European Symposium on Optics and Photonics for Defence and Security*, 2004, pp. 71-78.

[10]A. D. McAulay and J. Wang, "A Sagnac interferometer sensor system for intrusion detection and localization," in *Defense and Security*, 2004, pp. 114-119.

[11]L. Jiang and R. Yang, "Identification technique for the intrusion of airport enclosure based on double Mach-Zehnder interferometer," *Journal of Computers*, vol. 7, pp. 1453-1459, 2012.

[12]X. Zhang, T. Liu, K. Liu, J. Jiang, Z. Ding, and Q. Chen, "Reducing location error and processing time of dual Mach-Zehnder interferometric fiber perturbation sensor using zero-crossing analysis," in *OFS2012 22nd International Conference on Optical Fiber Sensor*, 2012, pp. 8421A8-8421A8-4.

[13]S. Xie, M. Zhang, S. Lai, and Y. Liao, "Positioning method for dual Mach-Zehnder interferometric submarine cable security system," in *SPIE Defense, Security, and Sensing*, 2010, pp. 76770A-76770A-4.

[14]S. S. Mahmoud and J. Katsifolis, "Robust event classification for a fiber optic perimeter intrusion detection system using level crossing features and artificial neural networks," in *SPIE Defense, Security, and Sensing*, 2010, pp. 767708-767708-12.

[15] A. D. Kersey, M. J. Marrone, and A. Dandridge, "Observation of input-polarization-induced phase noise in interferometric fiber-optic sensors," *Optics letters*, vol. 13, pp. 847-849, 1988.